Paper No.
2764

Experimental Study of Concurrent Naphthenic Acid and Sulfidation Corrosion

Vijaya. Kanukuntla, Dingrong Qu, Srdjan Nesic,
Institute for Corrosion and Multiphase Technology
Ohio University
342 West State Street, Athens, Ohio 45701

Alan Wolf
ExxonMobil Research and Engineering
1545 Rt 22E Room LB264, PO Box 998
Annandale, Clinton, NJ, 08801

ABSTRACT

Corrosion rates of mild steel (ASTM[(1)] A-106) and 5Cr (ASTM A-182 Grade F 5) exposed to a model oil containing naphthenic acids and sulfur species were studied at high temperature. The effects of test duration, temperature, total acid number, and total sulfur content were determined by the mass change method and by using SEM. Parallel tests were conducted in standard constant inventory autoclaves and a specially designed Flow Through Mini-Autoclave which enabled steady replenishment of the fluid.

It was found that the corrosion behavior of two steels did not differ significantly under all the test conditions covered in this study. Increasing the test duration beyond 24 hours did not affect the corrosion rates much, but increased the amount of corrosion scales found on the steel surface. Corrosion rates were independent of naphthenic acid concentration until reaching a threshold TAN value, and then increased sharply. Higher total sulfur content (0.38%) led to a higher threshold TAN value, which was attributed to the better sulfide scale protectiveness. For these low to moderate sulfur conditions, no correlation between scale thickness/porosity and the corrosion rate was found.

[(1)] ASTM International (ASTM), 100 Barr Harbor Dr., West Conshohocken, PA 19428-2959.

Key Words: Carbon steel, 5Cr, Naphthenic acid corrosion, sulfidation corrosion, corrosion scale

INTRODUCTION

Sulfidation corrosion and naphthenic acid corrosion have given rise to reliability and safety concerns in refinery distillation units for decades. Sulfidation corrosion is extensively observed as high temperature corrosion in refineries, and has been broadly studied. Lab tests [1,2] and refinery experience [3,4] have partially revealed the sulfidation corrosion mechanism. McConomy curves are commonly used to predict the relative corrosivity of crude oils and their various fractions due to sulfidation [5]. However, it is also found that knowing the sulfur content of the oil fraction is not always sufficient to predict the total corrosion rate. Since the real fractions may vary significantly with respect to the type of sulfur compounds [6,7] and may contain naphthenic acid, these parameters complicate their effect on corrosion.

The initial concern about naphthenic acid corrosion dates back to the previous century [8], and it keeps drawing attention of refineries today since. The, so called, "opportunity" crudes with a high naphthenic acid content are still being exploited and refined[9]. Effects of temperature [10], metallurgy [11], TAN [12], and local flow conditions [13] have been extensively investigated. Naphthenic acid corrosion is complicated not least because of the complexity of the naphthenic acid compounds found in crudes from the various sources. Sometimes, the distribution of naphthenic acids is grouped according to their boiling point, with an implication that naphthenic acids with different boiling points lead to different corrosivity [14].

Concurrent presence of both sulfur containing compounds and naphthenic acids in crudes introduces a new level of complexity into the study of the corrosion mechanisms. Sulfidation corrosion leads to formation of a sulfide scale, which provides some degree of protection against naphthenic acid corrosion, however this subject has been given relatively little systematic attention in the past.

In the present study, tests were done with *model* oil fractions which have a relatively "simple" and easily reproducible composition when it comes to the sulfur compounds and naphthenic acids. In the experiments, the corrosion rate and scale information were evaluated as functions of the test duration, temperature and concentration of corrosive species. The generic corrosion mechanisms derived from this study which was based on model oil compounds could be extrapolated to many other systems involving real oil fractions, given some additional testing and adjustments.

EXPERIMENTAL DESIGN

Materials and media

The test fluids in this study include various mixtures of a *yellow* (e.g. lightly hydrofined and no acid content) oil, a *white* oil (referred to below as Tufflo) and a commercially available rather pure mixture of naphthenic acids (denoted below as NAP). The yellow oil has 0.38% total sulfur content and no naphthenic acid. NAP has a Total Acid Number (TAN) of 228 mg KOH/g, but low sulfur content. Tufflo has negligible sulfur content and no naphthenic acids. The test fluids were prepared by "spiking" the yellow oil with Tufflo and NAP to achieve the desired total sulfur content and TAN.

Two steels, a mild steel (denoted below as CS) and a 5%Cr steel (denoted below as 5Cr), were used to evaluate their corrosion rate and scale formation rate. All coupon surfaces were ground to 600-grit by sand paper, and cleaned and degreased in acetone and dried immediately before corrosion tests. The original coupon weights were measured and recorded (W_0). Three coupons made from carbon steel and three made from 5Cr steel were used in each experiment. Two coupons from each steel were used to measure the weight change i.e. to determine the corrosion rate and scale formation rate, while the third one was used for surface and cross-section analysis.

Apparatus and procedures

A battery of standard autoclaves was used in this study. The autoclave tests provided basic information under all conditions. However, since the test media could not be changed during the whole test duration ("constant inventory test"), there was a concern about the thermal decomposition of naphthenic acids and sulfur compounds as well as accumulation of corrosion products. Therefore, a special designed apparatus: Flow Through Mini-Autocalve (FTMA), was also used to avoid this problem, which had a small but continuous flow of fresh test media through the system. Other than that, due to a very slow fluid refreshment rate, the FTMA tests were assumed to be equivalent to stagnant flow corrosion tests performed in autoclaves.

After the tests, coupons which had a corrosion scale were removed from the test equipment, rinsed with toluene and acetone, dried, and then weighed. This weight was recorded as W_{Rinse}. The coupons were mechanically scrubbed with a stiff plastic brush while wetted (using isopropyl alcohol) to remove any loose scale, and then dried and weighed again. This weight was recorded as W_{Rub}. After that, an ASTM G1 Clarke solution was used to dissolve the remaining scale, and the coupons were dried and weighed again. This last step was repeated if needed a few times until no change in the weight was measurable. This weight was recorded as W_C.

The corrosion rate (CR) in mm/y was calculated as follows:

$$CR_{mm/y} = \frac{W_0 - W_C}{A \cdot t \cdot \rho_{steel}} \cdot 24 \cdot 365 \cdot 1000 \quad (1)$$

where:

W_0 : original coupon weight in kg;
W_C : final coupon weight in kg;
A : area in m^2;
t : test duration in hr;
ρ_{steel} : steel density in kg/m^3.

However, corrosion rates presented were normalized on a consistent basis enabling cross-figure comparisons according to the company confidentiality policy.

Assuming a 100% dense FeS, a theoretical total scale thickness (H_T), and adherent scale thickness (H_A) in μm could be theoretically calculated by:

$$H_T = \frac{W_{Rinse} - W_C}{A \cdot \rho_{FeS}} * 10^6 \quad (2)$$

$$H_A = \frac{W_{Rub} - W_C}{A \cdot \rho_{FeS}} * 10^6 \quad (3)$$

Where:

W_{Rinse} : rinse weight in kg;
ρ_{FeS} : FeS density in kg/m^3;
W_{Rub} : Rub weight in kg.

Since one coupon from every test for each steel was cross sectioned and used for SEM observation, the actual measured scale thickness (H_M) in μm was obtained. The porosity of scale (η) in % was then calculated as:

$$\eta = (1 - \frac{H_T}{H_M}) \cdot 100\% \quad (4)$$

RESULTS

Time history

Figure 1 shows the time history of corrosion rate and adherent scale thickness in oil with 0.1 TAN and 0.38% total sulfur at 650°F (343°C). For FTMA tests, corrosion rates of both CS and 5Cr started out higher, but rapidly decreased in the first 24 hours, and then leveled off (Figure 1(a)). The reduction of corrosion rates could be ascribed to the growth of the protective sulfide scale layer. Notice that corrosion rates of both CS and 5Cr were approximately the same under all test conditions.

For autoclave tests, after 3 hours the same corrosion rates were observed as for the FTMA indicating good repeatability and compatibility of the two experimental systems. Beyond 3 hours, the protective sulfide scale layers grew in autoclaves in a similar fashion as was seen in the FTMA, which retarded the corrosion. However, in the autoclaves aggressive H_2S accumulated due to the thermo-decomposition of sulfur compounds.

As mentioned previously, both the total scale thickness and the adherent scale thickness were calculated. Adherent scale is the focus here as it was believed to be much more protective than the loose outer scale layer, which was easily mechanically removed. When comparing the two series of experiments, for short exposures (3 and 6 hours) the coupons exposed in the FTMA and autoclaves had approximately the same adherent scale thickness (Figure 1(b)). However, with the increase of test time, the adherent scale thickness for autoclave samples grew much faster than that in the FTMA. This difference was attributed to the accumulation of aggressive H_2S in autoclave which led to faster sulfidation. When comparing, the adherent scale thickness for CS and 5Cr did not show any significant difference in any given test.

Figure 2 to Figure 5 show the surface morphology and cross section image of CS coupons exposed in the FTMA for different test times. After 6 hour of exposure, the surface morphology of the scale clearly displayed the polishing lines generated during sample preparation (Figure 2(a)). Corresponding cross section image showed a multi-layer structure of the sulfide scale. The outer layer was composed of columnar sulfide crystals (Figure 2(b)). Underneath the outer layer, there was another loose layer composed of large sulfide crystals, and a finer more compact one below it. After 24 hour test exposures (Figure 3(a)), the polishing lines are still visible in the surface scale morphology. Inter-connected cracks were also observed, as well as a multi-layer structure as shown in Figure 3(b). Scale detachment and cracks were observed in even longer exposures (48 hours) as shown in Figure 4(a). The cross section image shown in Figure 4(b) shows a mostly compact inner scale layer. For 96 hour exposures, the coupon surface morphology did not show many loose outer scales (Figure 5(a)). The corresponding cross section image showed both vertical cracks and horizontal delamination (Figure 5(b)).

Figure 6 to Figure 9 show the surface morphology and cross section image for the 5Cr steel exposed in the FTMA for different test times. SEM images for 5Cr were similar to what was observed on CS. The coupons exposed in the autoclaves had displayed similar scale morphologies and therefore they are not showed here.

Temperature dependency

Figure 10 shows the temperature effect on the corrosion rate and the adherent scale thickness in oil with 0.1 TAN and 0.38% total sulfur in 24 hour long tests. Corrosion rates for both CS and 5Cr increased invariably with test temperature (Figure 10(a)), with a higher rate in autoclaves when compared to the FTMA. An attempt was made to plot the natural logarithm of normalized corrosion rates against the reciprocal of absolute temperature (Figure 10(b)). The slopes of the fitted lines are summarized in Table 1 indicated that the corrosion kinetics obeyed the Arrhenius law. In FTMA, the apparent activation energies of the overall corrosion reaction on CS and 5Cr were similar, around 55

kJ/mol. Several possible reasons made the apparent activation energies in autoclave appear higher, 98 and 123 kJ/mol respectively. Primarily, a thicker scale which formed on the autoclave exposed samples, led to higher apparent activation energies. Figure 10(c) shows that increasing temperature also increased the adherent scale thickness. Also, the closed autoclave system prevents escape of H_2S which may increase corrosion compared to the FTMA which permits the gas to escape.

Figure 11 shows a typical temperature effect on CS surface scale morphology. At 550 °F (288°C), the surface was covered by a fine, compact iron sulfide scale (Figure 11(a)). Figure 11(c) shows surface morphology at 650 °F (343°C). A loose, porous scale covered the whole surface, with many cracks in it.

TAN dependency

Figure 12 shows the TAN dependency in oil with 0.38% total sulfur, for a 24 hour exposure at 650 °F (343°C). For the FTMA, the corrosion rates for both CS and 5Cr remained constant between TAN of 0.1 and 2 and then increased sharply when TAN increased from 2 to 4 (Figure 12(a)). This result indicated that the corrosion mechanism changed from sulfidation corrosion dominated to naphthenic acid corrosion dominated after the critical TAN was exceeded. For autoclave tests, the corrosion rates for both CS and 5Cr remained constant until TAN 4, and then sharply increased when TAN increased from 4 to 5.

In the FTMA exposures, the adherent scales remained constant until TAN 2, and then decreased to almost zero for higher TAN (Figure 12(b)). In autoclave exposures the amount of scale was constant up to TAN 4, and then increased greatly for higher TAN. However, this did not result a better protection against naphthenic acid corrosion. This discrepancy indicates that the adherent scale thickness is not a good indicator for scale protectiveness.

Typical surface morphologies and scale cross section images for CS coupons exposed in autoclaves at different TAN are shown in Figure 13 to Figure 15. Surface morphology for a TAN 2 exposure is shown in Figure 13(a). The corresponding cross section morphology is presented in Figure 13(b). Figure 14 shows a multi-layer structure obtained in the TAN 3 test. The porous outer layer and the compact layer underneath are visible in Figure 14(a). The cross section image shows a multilayer structure (Figure 14(b)). For a TAN 5 test, the image in Figure 15 shows a porous outer scale with large voids.

Effect of sulfur containing compounds

Figure 16 and 17 shows the effect of total sulfur content in the oil by comparing 0.15% and 0.38% total sulfur series tests. A transition from Sulfidation to naphthenic acid dominated corrosion regime was also found in both the FTMA and autoclave tests for CS (Figure 16(a)). Changing total sulfur from 0.38% to 0.15% affected the critical TAN value which changed from 2 to 1.6 in FTMA, and from 4 to 3 in autoclaves. Both set of results indicate that higher total sulfur content led to better scale protectiveness. Again, there was no correlation between adherent scale thickness and the corrosion rate. Very similar conclusions could be drawn from the 5Cr results in both the FTMA and autoclaves (Figure 17).

DISCUSSION

Protectiveness of iron sulfide scale and corrosivity of naphthenic acid

Corrosion in refineries above 500°F (260°C) was basically defined as a combination of sulfidation corrosion and naphthenic acid corrosion. Sulfur containing species in oil are often corrosive; however, their corrosion product, iron sulfide scale may be protective. The type of sulfur species [6], the

concentration of sulfur compounds, and the metallurgy [11] were all common factors known to affect sulfidation corrosion. In the present study, the sulfur species type and their origin were maintained as a constant to avoid excessive complexity associated with sulfidation. Concentration of sulfur compounds was changed in a rather limited range, from 0.15% to 0.38%. Pure sulfidation corrosion rates were comparable under these two concentrations (for both CS and 5Cr steel), and probably acceptable for refineries in the long run. However the issue is whether one could rely on the sulfide scale for protectiveness against naphthenic acid corrosion. It was found that oil with 0.38% total sulfur provided better protectiveness against naphthenic acid attack when compared to the 0.15% total sulfur containing oil.

Temperature, metallurgy, TAN, molecular structure [15], and local flow conditions are known to be important factors affecting naphthenic acid corrosion. In this study, the metallurgy (CS vs. 5Cr steel) did not appear to lead to significant differences when it comes to naphthenic acid corrosion. In all cases the corrosivity increased significantly with TAN value above a certain threshold value. At low TAN, under the so-called sulfidation dominated regime, changing TAN does not affect naphthenic acid corrosivity, because the corrosion process is controlled by the protectiveness of the iron sulfide scale. The critical TAN value increased for oils with higher total sulfur content.

Correlation between scale thickness, scale porosity and corrosion rate

As indicated above, there was no correlation between scale thickness and corrosion rate. It is worthwhile examining porosity, which is a ratio of the volume of voids in the scale and the total scale volume. Figure 18 shows porosity vs. normalized corrosion rate with time and TAN (obtained in autoclaves). It can be seen that scale porosity is also not a good indicator for scale protectiveness. The investigation trying to assess these results is continuing.

CONCLUSION

Two parallel series of experiments conducted in rather different experimental setups were used to study concurrent naphthenic acid and sulfidation corrosion. In general the results from the two series were in agreement. The following conclusions can be drawn:

1. The accumulation of corrosive H_2S in constant inventory autoclave tests makes them significantly different from those obtained in the FTMA, which enables continuous flushing. This effect is aggravated with time and particularly for oils with higher total sulfur content and at higher temperature. Therefore caution is advised when conducting autoclave tests under these conditions.
2. Corrosion rates remained constant with increasing TAN until a critical value was reached, which was a function of the oil total sulfur content. At higher TAN, the corrosion rate increased sharply marking a transition from sulfidation to naphthenic acid dominated corrosion regime.
3. Increasing oil total sulfur content from 0.15% to 0.38% did not affect the long term pure sulfidation corrosion rates, however it resulted in a higher critical TAN value for sulfidation/acid transition.
4. While the presence of an iron sulfide scale was clearly protective, neither the scale thickness nor porosity showed a good correlation with the measured corrosion rates.

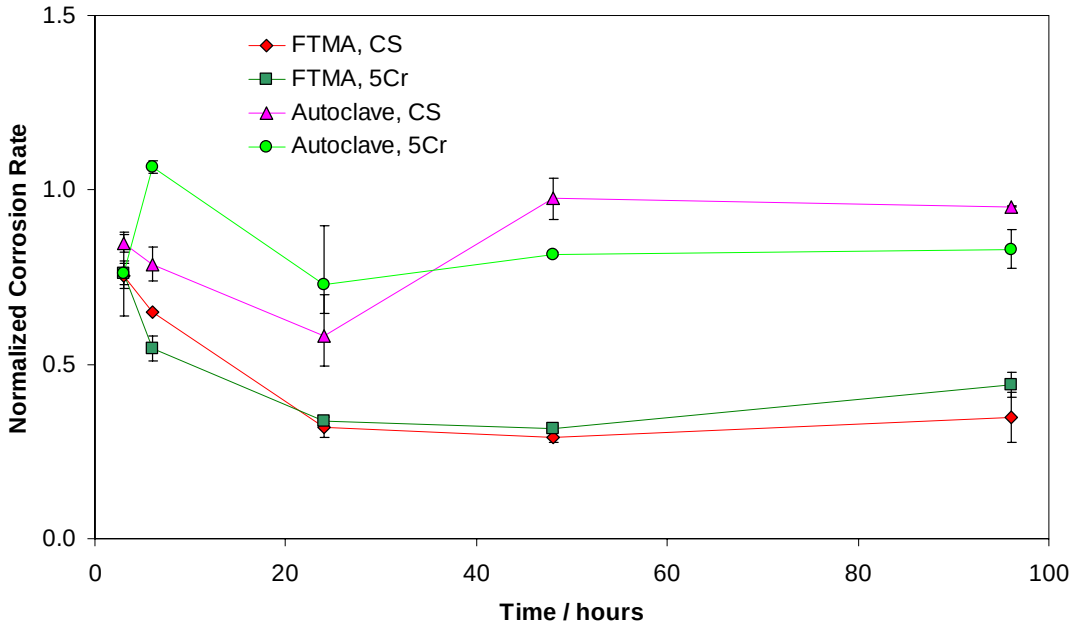

(a)

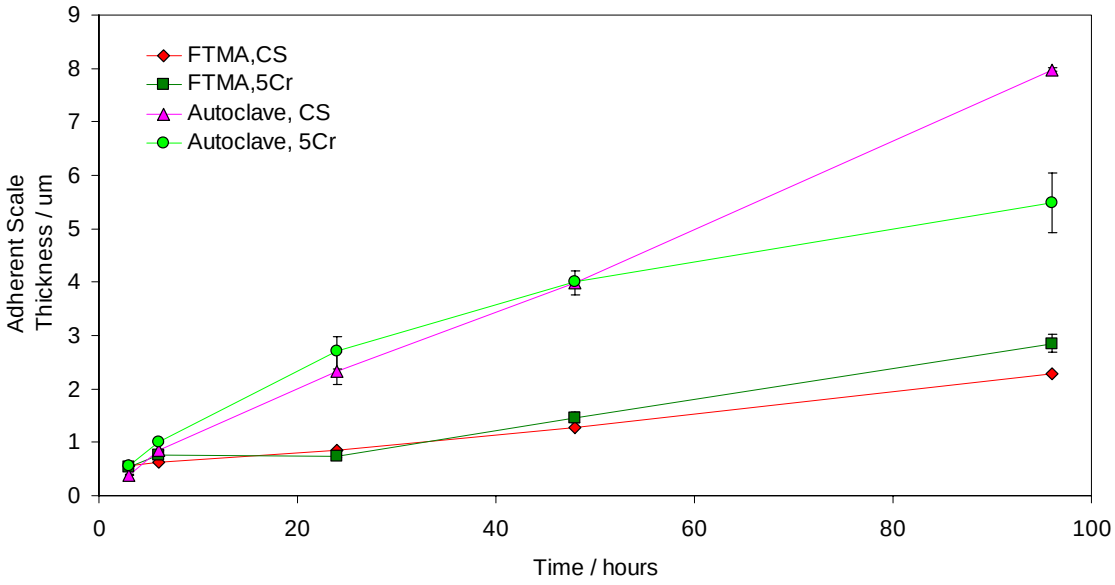

(b)

FIGURE 1. Time history results in oil with 0.1 TAN and 0.38% total sulfur at 650°F (343°C); (a) corrosion rate, (b) adherent scale thickness. Corresponding surface analysis and cross sectional images of FTMA coupons can be viewed from Figure 2 to Figure 9.

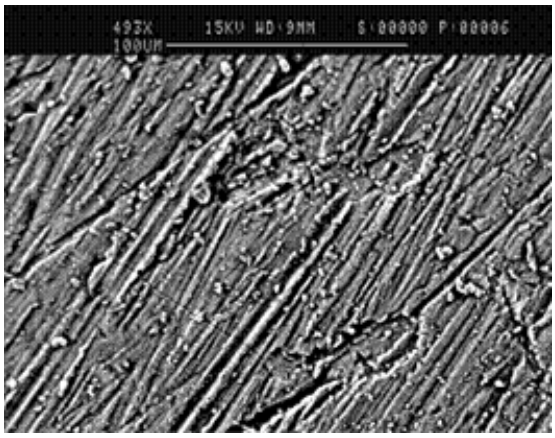

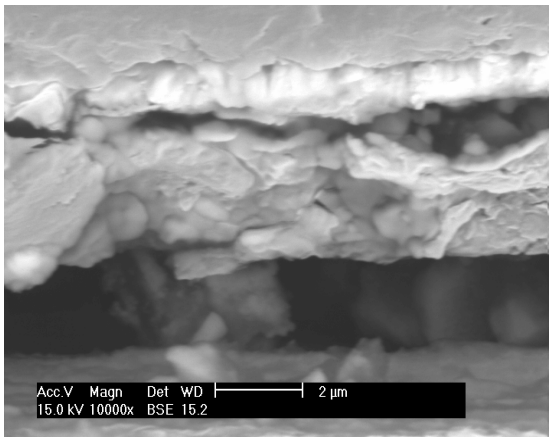

(a) (b)

FIGURE 2. Surface morphology (a) and cross section view (b) of FTMA CS coupon exposed to oil with 0.1 TAN and 0.38% total sulfur at 650°F (343°C) temperature and 6 hour test period.

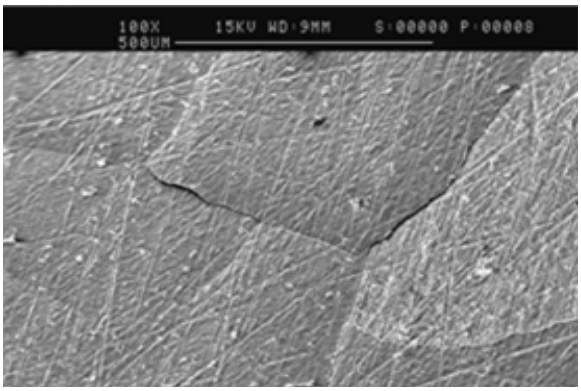

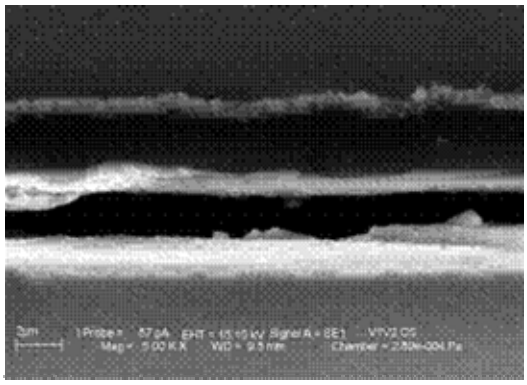

(a) (b)

FIGURE 3. Surface morphology (a) and cross section view (b) of FTMA CS coupon exposed to oil with 0.1 TAN and 0.38% total sulfur at 650°F (343°C) temperature and 24 hour test period.

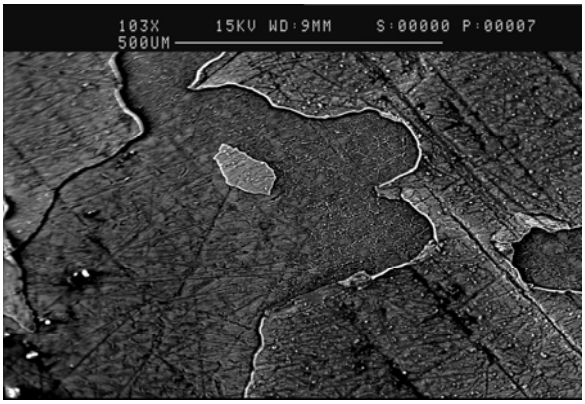

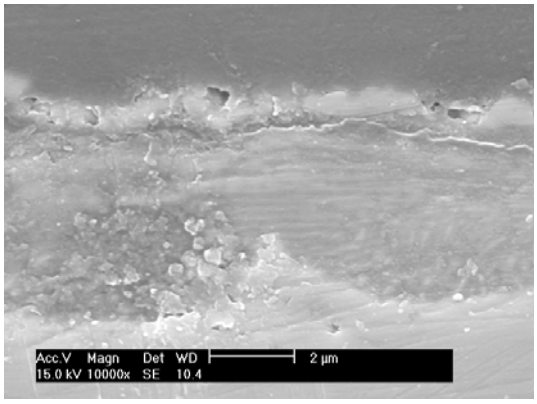

(a) (b)

FIGURE 4. Surface morphology (a) and cross section view (b) of FTMA CS coupon exposed to oil with 0.1 TAN and 0.38% total sulfur at 650°F (343°C) temperature and 48 hour test period.

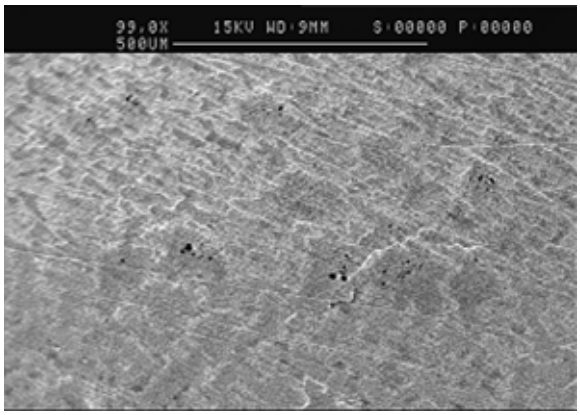

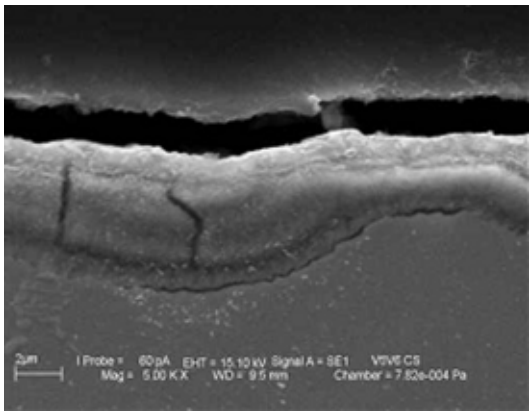

(a) (b)

FIGURE 5. Surface morphology (a) and cross section view (b) of FTMA CS coupon exposed to oil with 0.1 TAN and 0.38% total sulfur at 650°F (343°C) temperature and 96 hours test period.

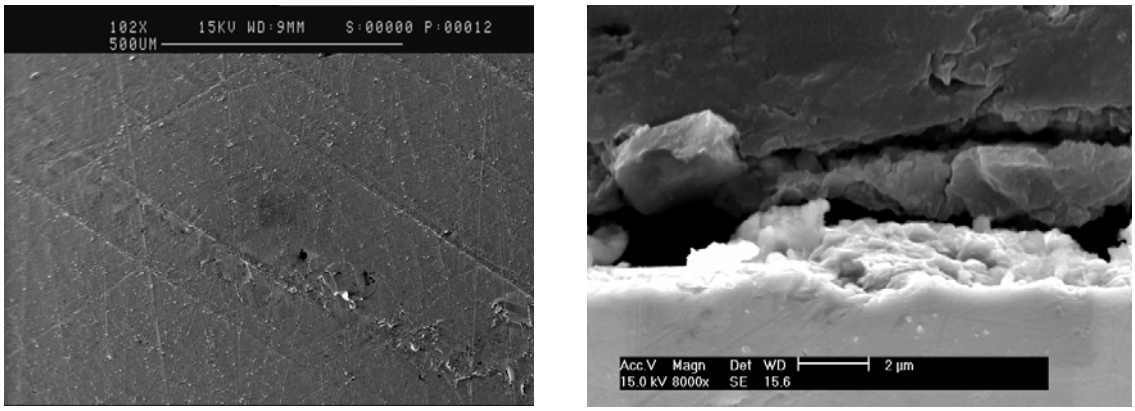

(a) (b)

FIGURE 6. Surface morphology (a) and cross section view (b) of FTMA 5Cr coupon exposed to oil with 0.1 TAN and 0.38% total sulfur at 650°F (343°C) temperature and 6 hour test period.

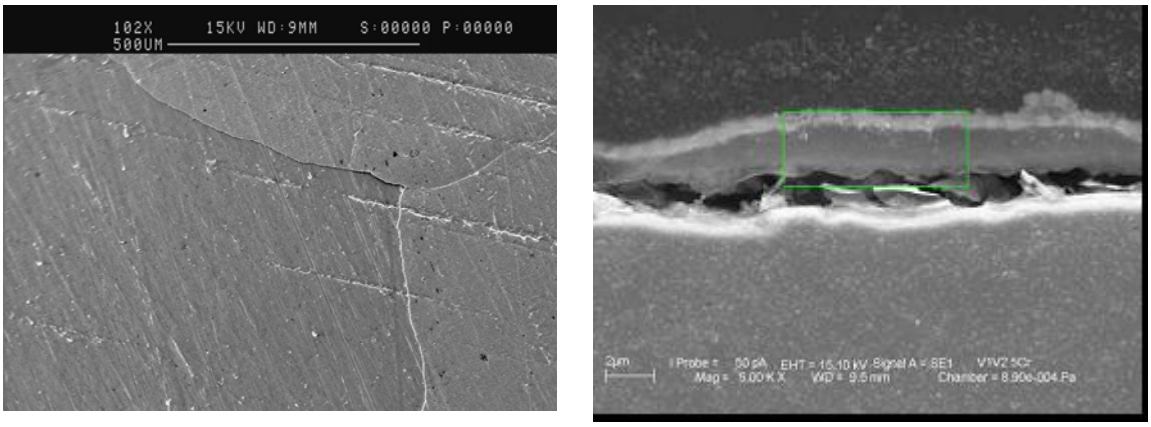

(a) (b)

FIGURE 7. Surface morphology (a) and cross section view (b) of FTMA 5Cr coupon exposed to oil with 0.1 TAN and 0.38% total sulfur at 650°F (343°C) temperature and 24 hour test period.

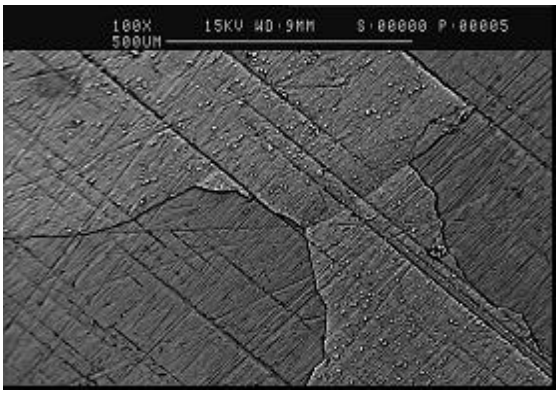

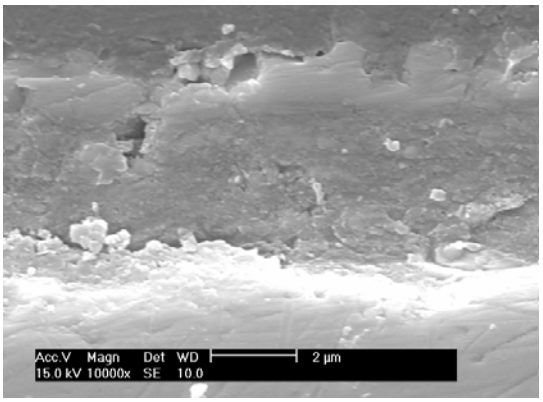

(a) (b)

FIGURE 8. Surface morphology (a) and cross section view (b) of FTMA CS coupon exposed to oil with 0.1 TAN and 0.38% total sulfur at 650°F (343°C) temperature and 48 hour test period.

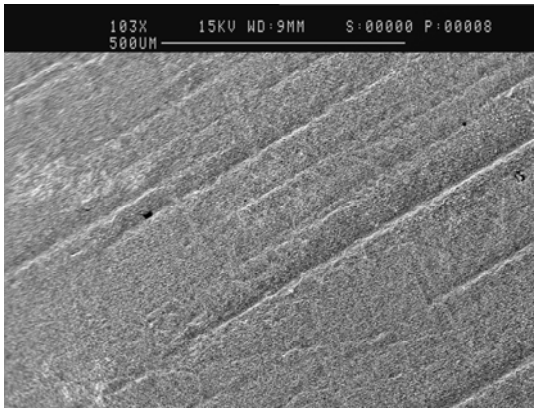

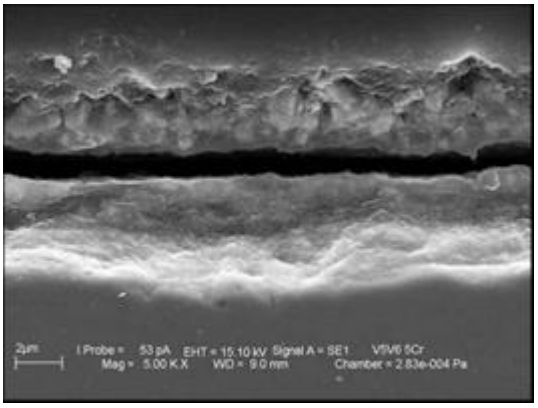

(a) (b)

FIGURE 9. Surface morphology (a) and cross section view (b) of FTMA 5Cr coupon exposed to oil with 0.1 TAN and 0.38% total sulfur at 650°F (343°C) temperature and 96 hours test period.

\

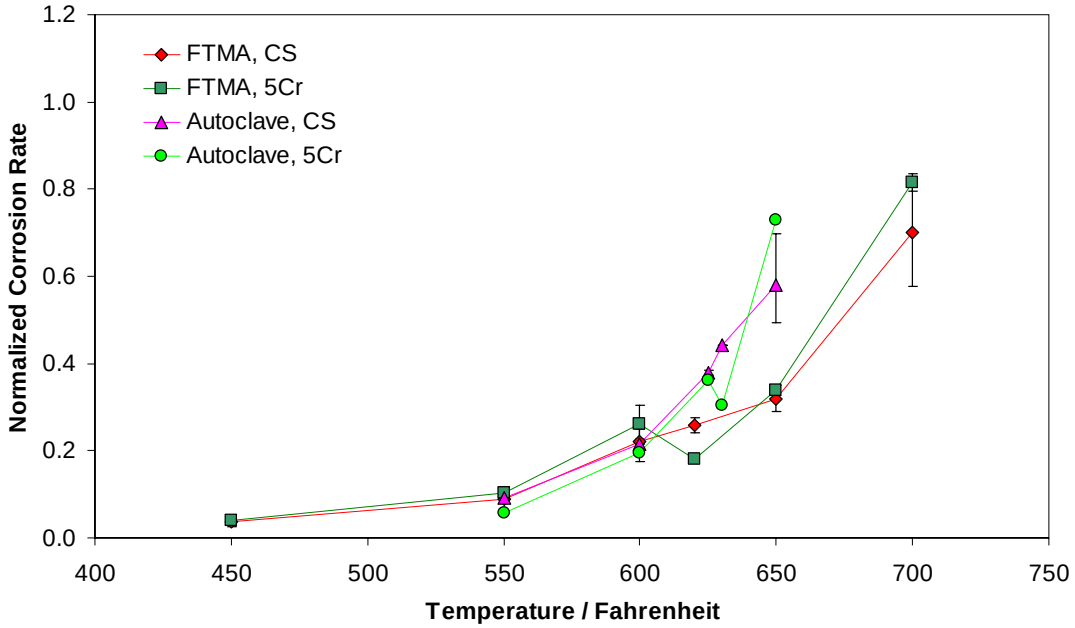

Figure 10 (a)

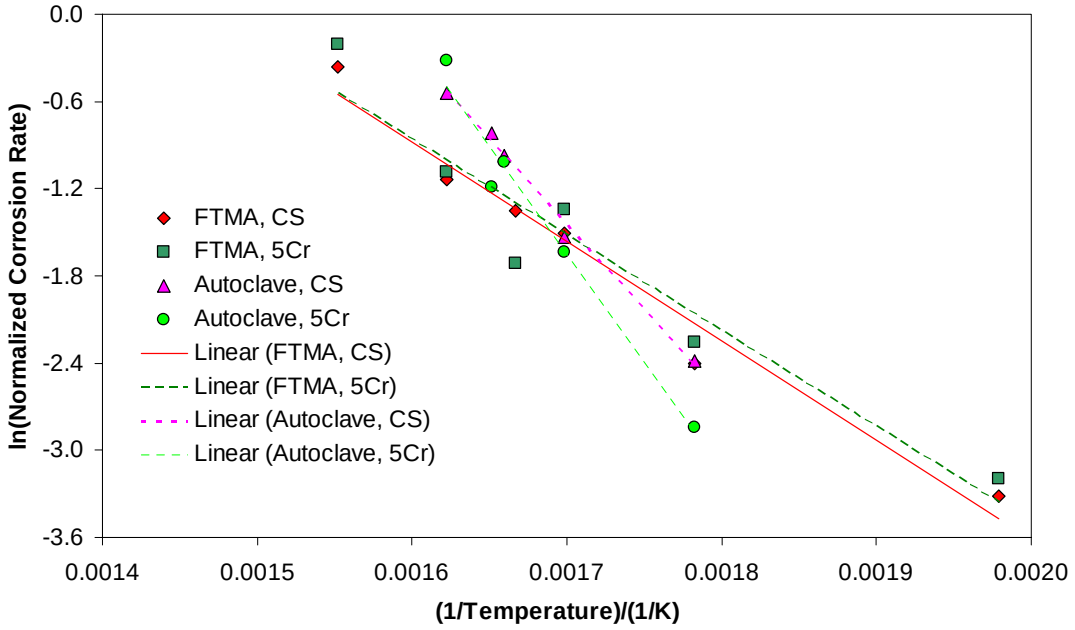

Figure 10 (b)

\

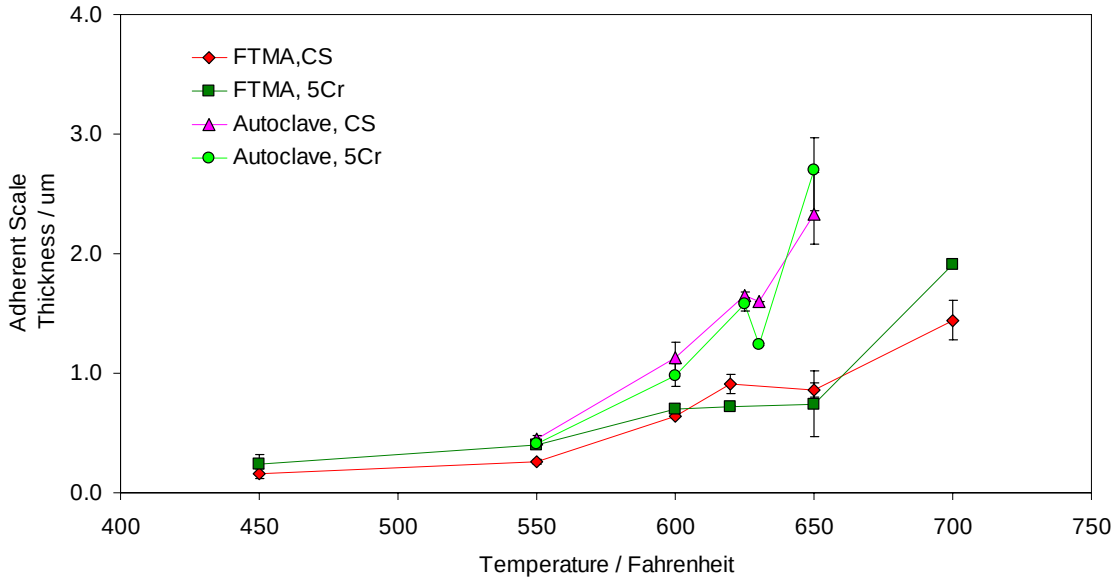

Figure 10 (c)

FIGURE 10. Temperature dependency results in oil with 0.1 TAN, 0.38% total sulfur, at 24 hours; (a) corrosion rate, (b) natural logarithm of normalized corrosion rates vs. the reciprocal of absolute temperature, (c) adherent scale thickness. Corresponding surface morphologies of autoclave CS coupons are shown in Figure 11.

TABLE 1. Linear fitting results for ln(CR) vs. 1/T. Corresponding plots are shown in Figure 10(b).

Equipment	Steel	Apparent Activation Energy / (kJ/mol)	R^2
FTMA	CS	56.9	0.97
FTMA	5Cr	54.9	0.93
Autoclave	CS	97.5	0.99
Autoclave	5Cr	123.3	0.97

\

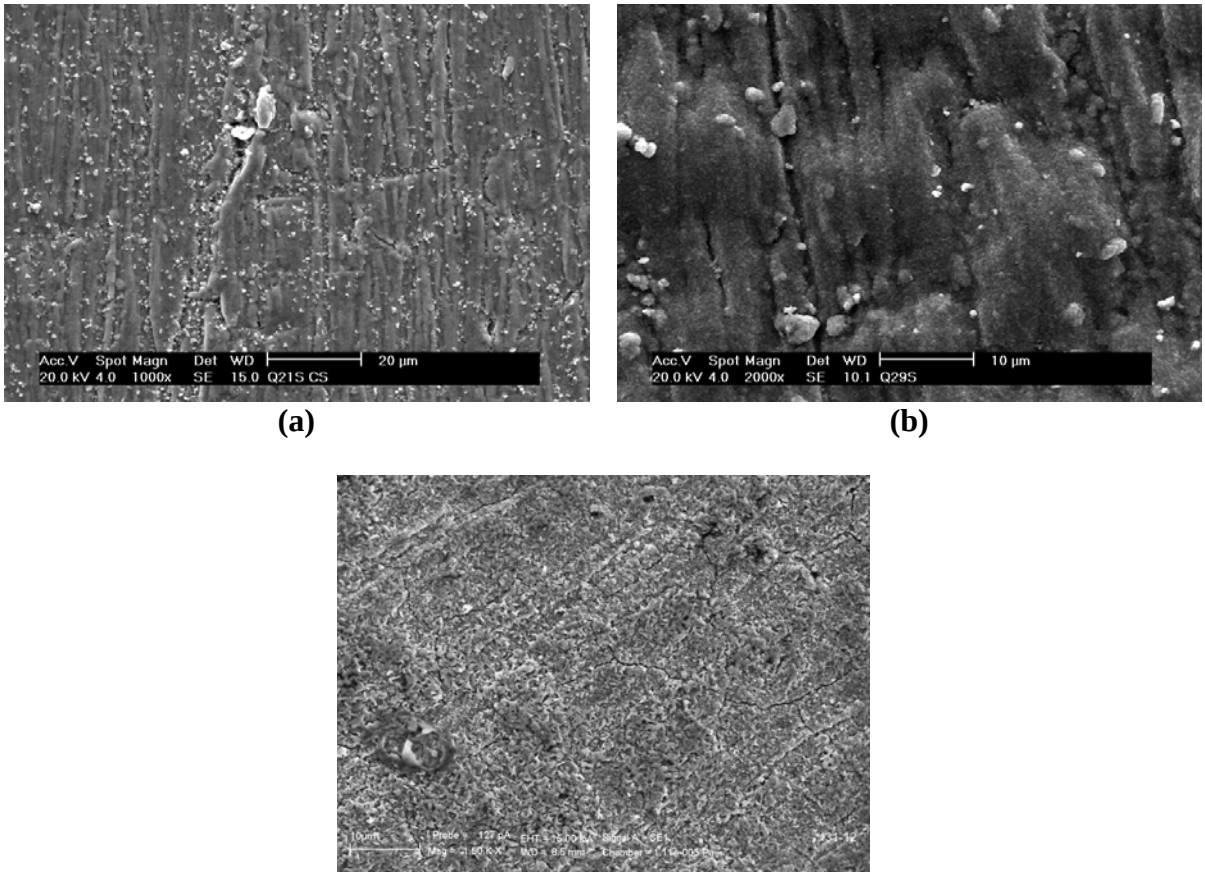

(a) **(b)**

(c)

FIGURE 11. Temperature effect on surface morphology of CS in oil with 0.1 TAN, 0.38% total sulfur at 24 hours; (a) 550 °F (288°C); (b) 600 °F (315°C); (c) 650 °F (343°C).

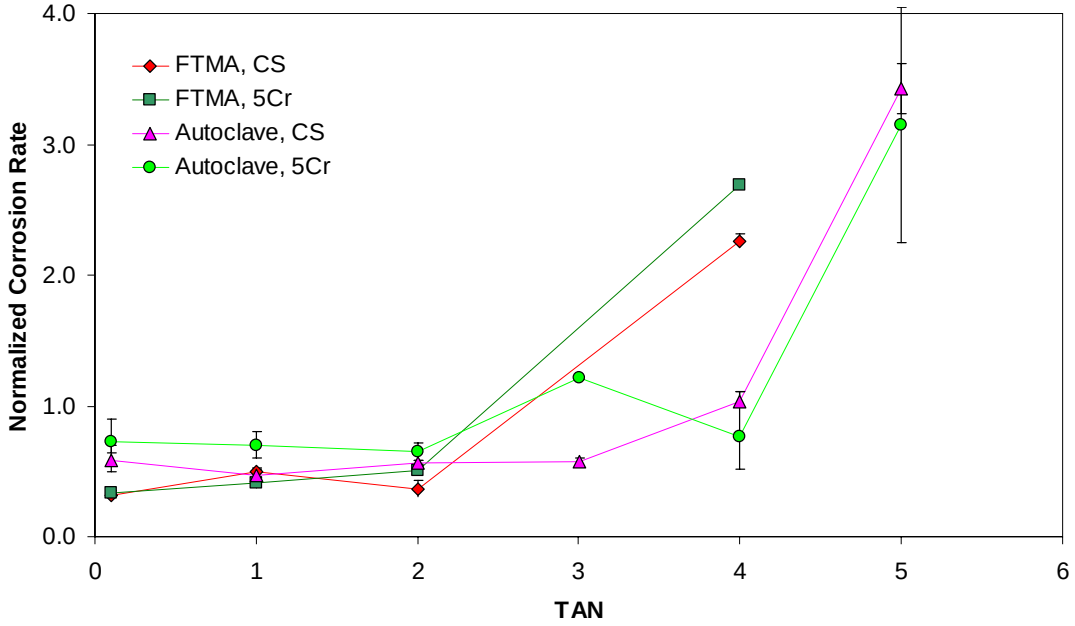

Figure 12 (a)

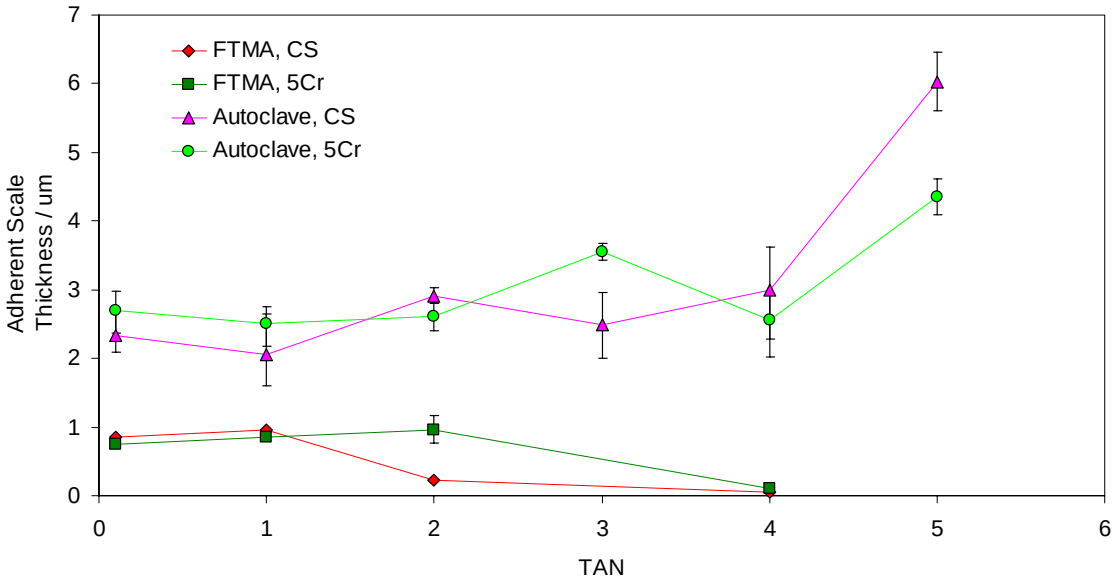

Figure 12 (b)

FIGURE 12. TAN dependency results in oil with 0.38% total sulfur, at 24 hours and 650 °F (343°C); (a) corrosion rate, (b) adherent scale thickness. Corresponding surface morphologies and cross section images of autoclave CS coupons are shown in Figure 13 to Figure 15.

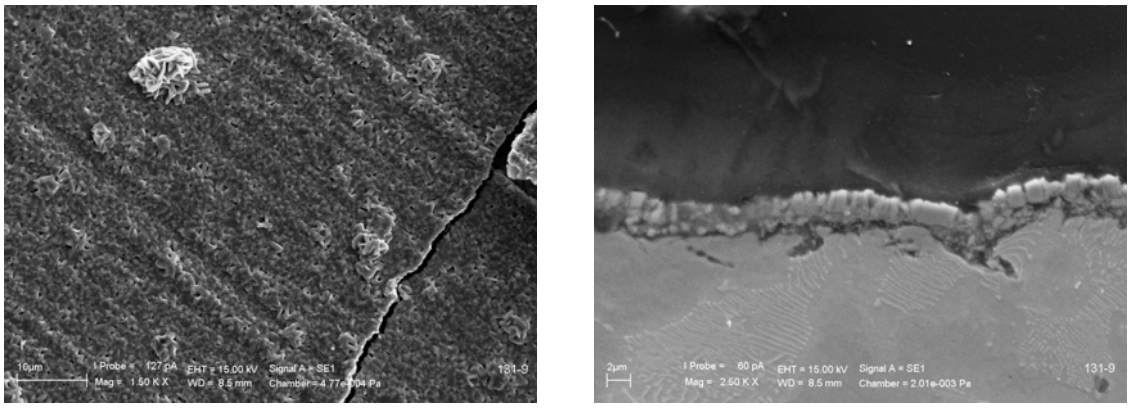

(a) **(b)**

FIGURE 13. (a) Surface morphology; (b) cross-section morphology of carbon steel coupon in oil with 2.0 TAN, 0.38% total sulfur, 650 °F (343°C) and 24 hours.

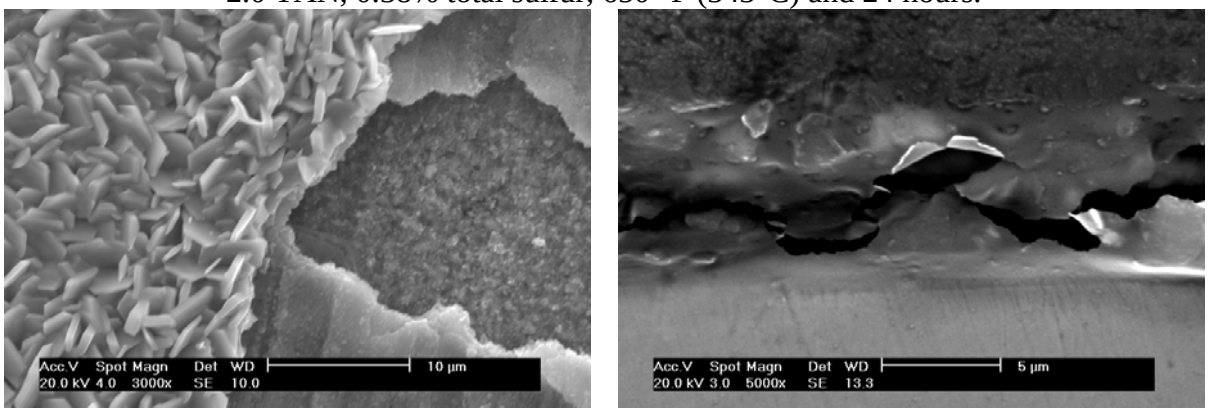

(a) **(b)**

FIGURE 14. (a) Surface morphology; (c) cross-section morphology of carbon steel coupon in oil with 4.0 TAN, 0.38% total sulfur, 650 °F (343°C) and 24 hours.

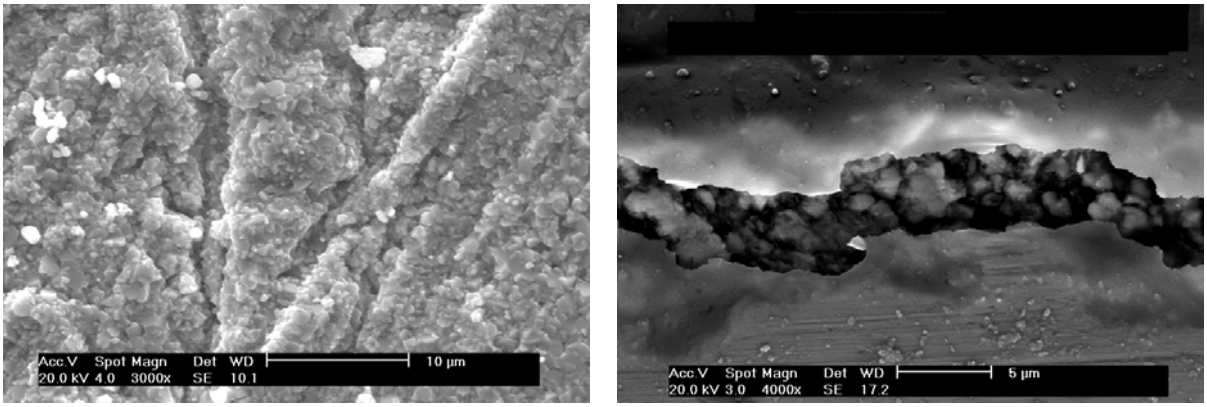

(a) **(b)**

FIGURE 15. (a) Surface morphology; (b) cross-section morphology of carbon steel coupon in yellow oil with 5.0 TAN, 0.38% total sulfur, 650 °F (343°C) and 24 hours.

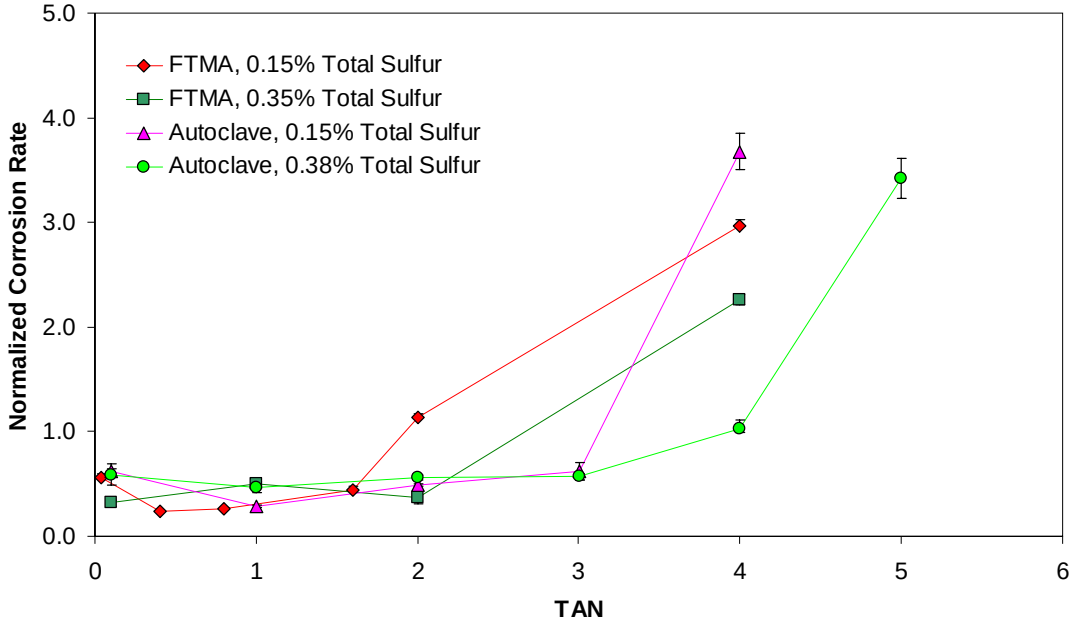

Figure 16 (a)

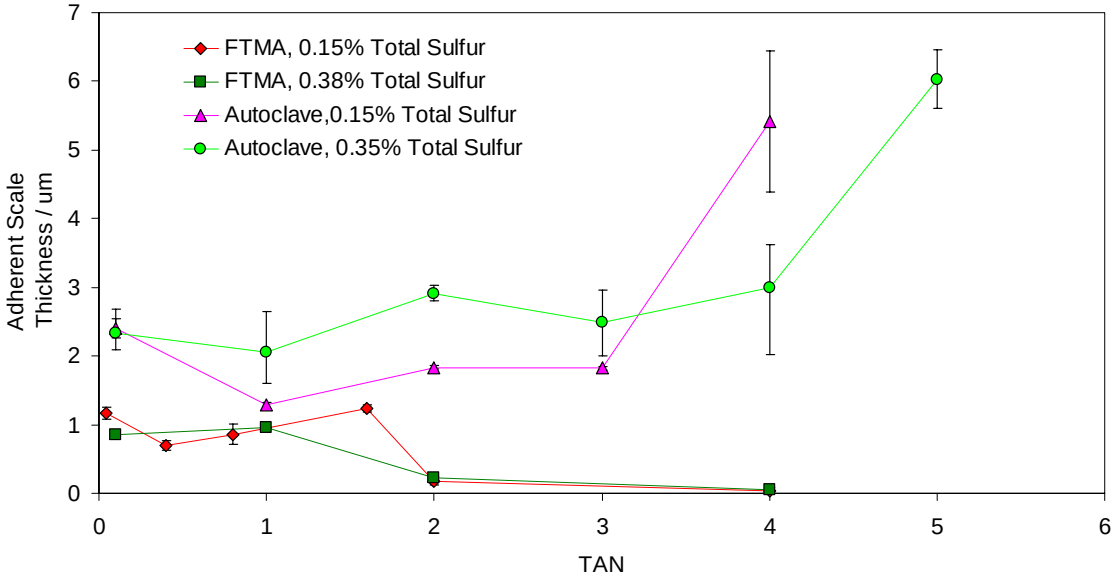

Figure 16 (b)

FIGURE 16. Total sulfur effect on CS in oil under 650 °F (343°C) at 24 hours with varied TAN; (a) corrosion rate, (b) adherent scale thickness.

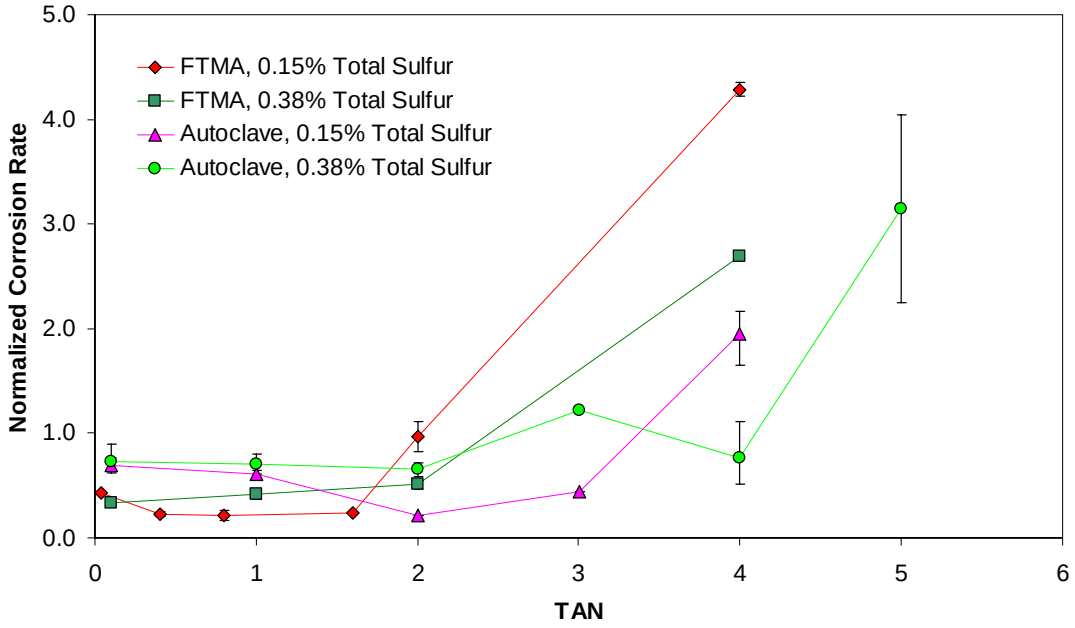

Figure 17 (a)

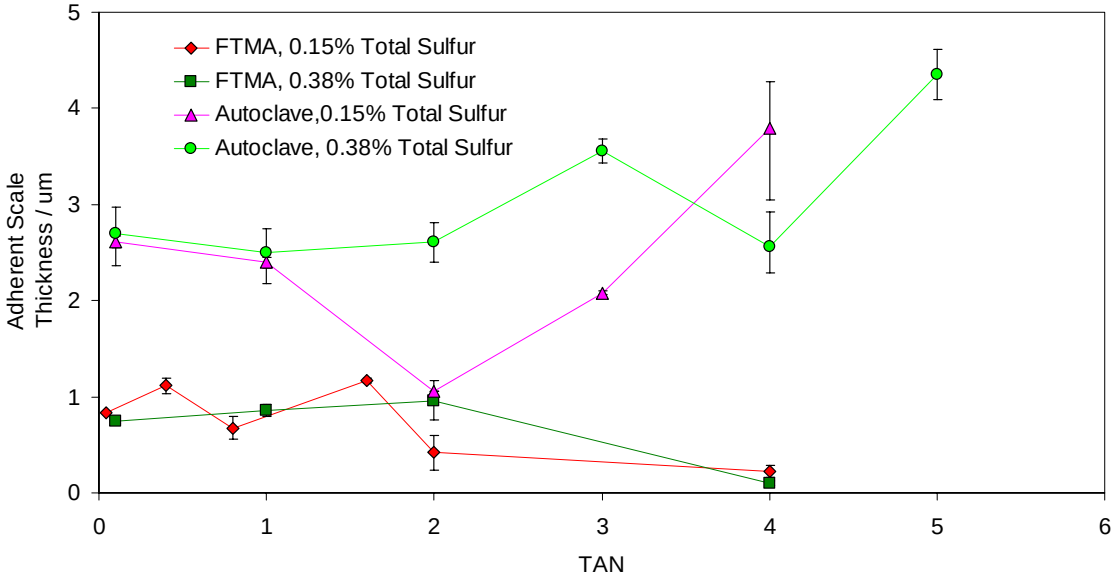

Figure 17 (b)

FIGURE 17. Total sulfur effect on 5Cr in oil under 650 °F (343°C) at 24 hours with varied TAN; (a) corrosion rate, (b) adherent scale thickness.

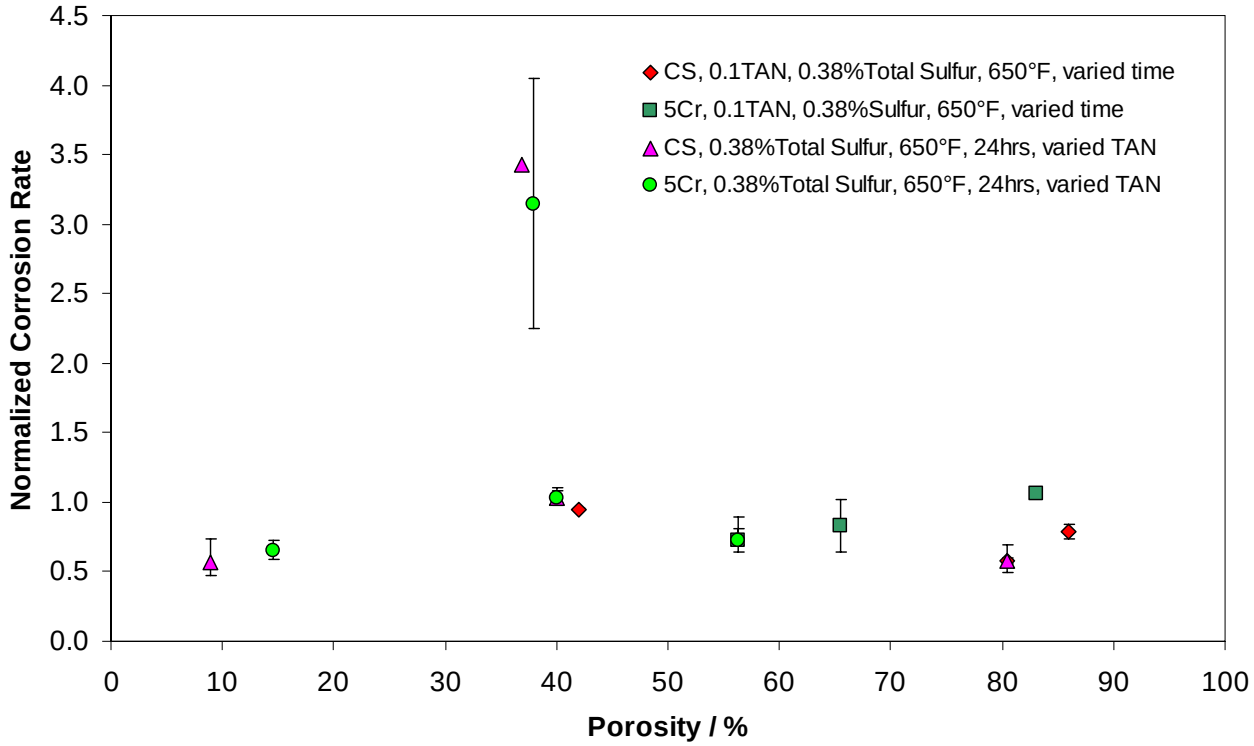

FIGURE 18. Porosity vs. Normalized Corrosion Rate for time history and TAN series results obtained in autoclave.

REFERENCES

1. Jorge L. Hau, Omar Yepez, Maria Isabel Specht, and Robert Lorenzo, "The Iron Powder Test for Naphthenic Acid Corrosion Studies", NACE CORROSION/99, Paper No.379
2. SaadedineTebbal, RussellD. Kane, and Kazuo Yamada, "Assessment of the Corrosivity of Crude Fractions from Varying Feedstock", NACE CORROSION/97, Paper No.498, 1997, 1-13.
3. Cathleen Shargay, Karly Moore, and Richard Colwell, "Survey of Materials in Hydrotreater Units Processing High TAN Feeds", NACE CORROSION/2007, Paper No.07573, 2007, 1-11.
4. Frank W.H. Dean, and Stephen W. Powell, "Hydrogen Flux and High Temperature Acid Corrosion", NACE CORROSION/2006, Paper No.06436, 2006, 1-9.
5. H. F. McConomy, "High-Temperature Sulfidic Corrosion in Hydrogen Free Environment," presented at the meeting of the Subcommittee on Corrosion during the 28th Midyear Meeting of the American Petroleum Institute's Division of Refining in Philadelphia, PA, May 1963.
6. Saadedine Tebbal, "Critical Review on Naphthenic Acid Corrosion", NACE CORROSION/99. Paper No.380.
7. K.R. Lewis, M.L. Daane, and R. Schelling, "Processing Corrosive Crude Oils", NACE CORROSION/99. Paper No.377.
8. W. A. Derungs, "Naphthenic Acid Corrosion – An Old Enemy of the Petroleum Industry", Corrosion 1956, 12, 617-622.
9. D. Johnson, G. McAteer, and H. Zuk, "The Safe Processing of High Naphthenic Acid Content Crude Oils Refinery Experience and Mitigations Studies", NACE CORROSION/2003. Paper No.03645.
10. D.R. Qu, Y.G. Zheng, H.M. Jing, Z.M. Yao, and W. Ke, "High Temperature Naphthenic Acid Corrosion and Sulphidic Corrosion of Q235 and 5Cr1/2Mo Steels in Synthetic Refining Media", Corrosion Science 48 (2006) 1960–1985
11. Michael J. Zetlmeisl, "Naphthenic Acid Corrosion and Its Control", NACE CORROSION/96. Paper No.218.
12. Sergio D. Kapusta, Alex Ooms, Andrew Smith, Frans van den Berg, and William Fort, "Safe Processing of Acid Crudes", NACE CORROSION/2004. Paper No.04637.
13. D. R. Qu, Y. G. Zheng, H. M. Jing, X. Jiang, and W. Ke, "Erosion-corrosion of Q235 and 5Cr1/2Mo Steels in Oil with Naphthenic Acid and/or Sulfur Compound at High Temperature", Materials and Corrosion 2005 56(8):533-541

14. B. Messer, B. Tarleton, M. Beaton, and T. Phillips, “New Theory for Naphthenic Acid Corrosivity of Athabasca Oilsands Crudes”, NACE CORROSION/2004. Paper No.04634.
15. Ding-Rong Qu, Yu-Gui Zheng, Xiu Jiang, and Wei Ke, “Correlation between the corrosivity of naphthenic acids and their chemical structures”, Anti-Corrosion Methods and Materials, 54/4 (2007) 211–218